# Non-linear tradeoffs allow cooperation to evolve from Prisoner's Dilemma to Snow Drift

Lin Chao[1,*] & Santiago F. Elena[2,3]

[1]Section of Ecology, Behavior and Evolution, Division of Biological Sciences, University of California San Diego, La Jolla, California 92093-0116, USA.

[2]Instituto de Biología Molecular y Celular de Plantas, Consejo Superior de Investigaciones Científicas-Universidad Politécnica de Valencia, Ingeniero Fausto Elio s/n, 46022 Valencia, Spain.

[3]The Santa Fe Institute, 1399 Hyde Park Road, Santa Fe NM 87501, USA.

[*]Correspondence: lchao@ucsd.edu, sfelena@ibmcp.upv.es

The existence of cooperation or the production of public goods is a major evolutionary conundrum. Restricting the goods to kin or to reciprocating individuals is promoted as a solution, but that is inappropriate because the benefits are no longer public. Without kinship or reciprocation, the evolution of cooperation is limited by the Prisoner's Dilemma (PD) game, which drives cooperators to extinction and selects for defectors that produce fewer public goods. Here we use existing molecular and genetic information on RNA viruses to create a mathematical model for the evolution of cooperation as a function of group size. While diffusible gene products are public goods, group size is represented by the number of virions co-infecting a host cell. Our results show that if a virus' investment into replication versus making gene products conforms to a linear tradeoff, the viruses evolve into a monomorphic population that remains trapped by PD. However, if the tradeoff is non-linear and group size exceeds a threshold, selection is diversifying and the population bifurcates into a dimorphic state with lineages of ultra-defectors and ultra-cooperators. The modeling of a non-linear tradeoff and ultra-defectors was motivated by the existence of viral defective interfering (DI) particles, which are contracted viral genomes that lack coding regions and therefore gain an extra advantage by being smaller than defectors that make some public goods. If group size is further increased, the ultra-cooperators evolve to produce public goods at a maximum rate that matches the production evolved by kin selection. The emergence of ultra-defectors and ultra-cooperators in our model creates the Snow Drift (SD) game, which is the most advanced form of cooperation. Thus, our model shows that evolution can easily transition from PD to SD via the increase of group size. Although formulated for viruses, our model is easily adaptable to most biological systems.

RNA viruses are the ideal organisms for modeling the evolution of cooperation. Besides providing some accurate information on the dynamics of the process, the molecular mechanisms that drive it have been elucidated. They are as simple as possible, yet not simpler of a general case. All viruses are parasites that need to infect a host cell to reproduce. If a single virion infects a cell, kin selection is the agent of evolution because the progeny viruses are clonal. Kin selection may be uniquely important, if not actively enforced, in many RNA viruses because the first one or few viruses to infect a cell exclude the entry of others[1-3]. However, if a larger number of viruses are able to co-infect the same cell, a genetically less related interaction group emerges and opportunities for PD, SD, cooperation, and defection are created[4-6]. By increasing the group size of viruses co-infecting the same host cell, it has been possible to demonstrate experimentally that RNA viruses can evolve to be trapped by PD[7,8]. Additionally, the molecular control of replication and transcription in *Vesicular stomatitis virus* (VSV; genus *Rhabdovirus*, family Rhabdoviridae) (Fig. 1a), which we take as our idealized virus, offers a near perfect mechanism for modeling the tradeoff between defection and producing public goods[9]. The

molecular control in VSV DI particles was also key for evaluating the non-linearity of the tradeoff in ultra-defectors (Fig. 1b).

Our model accommodates a viral population of size $N$ that is randomly divided into $N/m$ groups of size $m \geq 1$, where each group represents viruses that co-infect the same host cell. For virologists, $m$ would correspond to multiplicity of infection[10,11]. Once inside a cell, a virus must tradeoff between replicating its own genome and producing gene products. This aspect of the tradeoff was assumed to be linear because replication and transcription in VSV viruses compete for the same initiation site (Fig. 1a). Thus, let $i$ and $1 - i$ represent the effort an individual virus allocates to replicating its own genome and making public goods (*e.g.*, proteins), respectively (with $i \in [0, 1]$). We assumed additionally that an individual virus $n$ in a group of size $m$ has access to $1/m$ of the host's resources and therefore is able to make only $i_n/m$ public goods and $(1 - i_n)/m$ genomes. This assumption is justified because many viral DIs, as per their name, interfere by reducing the total yield of wild type and defective genomes produced by a co-infection group[12-18]. The reduction has also been shown to be linear, *e.g.* it is $i = ½$ when co-infections groups are 50% wild type and 50% DI viruses[19]. After genomes and gene products are assembled into virions, a progeny of $b$ number of viruses is released and the model determines the final fitness of an individual virus as

$$w_n = b\frac{i_n/m}{g} \qquad [1]$$

where $g$ is the total number of genomes produced by the group of size $m$, $g = \sum_{n=1}^{m} i_n/m$. To determine the value of $b$, we note that while its value could be equal to the total amount of public goods produced by the group, namely $h = \sum_{n=1}^{m} (1 - i_n)/m$, it could be less than $h$ if insufficient genomes are made. If both $g$ and $h$ are scaled in molar units required to assemble a viable virus, then $b = \min(g, h)$. If $g > h$, the excess genomes are wasted and $h$ caps the number of viruses produced. *Vice versa* if $g < h$ then genomes are the limiting factor and public goods are produced in excess.

We modeled evolution by starting with a parent population of size $N$ with known or assigned values of $i$ and assembling $N/m$ random groups. By using equation [1], the fitness of each virus was determined. A progeny population was then created by sampling $N$ viruses from the parent population. Selection is imposed because the fitness values were used to weight the sampling process. The progeny was then assembled into $N/m$ groups to create the parent population for the next generation. By using equation [1] and the weighted sampling, the process can be repeated to create new progeny and parent populations for as many generations as needed. If desired, the values of $i$ were mutated before selection.

The evolution of cooperation was monitored by modeling and tracking the values of $i$ over time in the population. By allowing the value of $i$ to change through mutations, the evolutionary dynamics of cooperation was followed to search for steady state outcomes. A first test was to model evolution with $m = 1$, for which an evolved optimum $i_k = ½$ was anticipated, and observed, because each group is clonal and kin selection between groups favors viruses that make equi-molar amounts of genomes and gene products (Fig. 2a). Thus, we used $i_k = ½$ as the evolutionary starting point and examined the effect of increasing $m$. In all cases $i$ evolved dynamically to higher steady state values as $m$ was increased (Fig. 2b). Because all of the populations remained monomorphic, we were able to determine analytically the steady state values by solving for the $i$ that maximized individual fitness in a group of $mi$ identical viruses (see Methods for the analytical derivation; equation [M3]). The solution

$$i_a = 1 - 1/m \qquad [2]$$

matched closely all of the steady state values evolved with the model (Fig. 2c). It is also an evolutionarily stable strategy (ESS) because mutants with either higher or lower values of $i$ have a lower fitness and cannot invade (see Methods). Note that if $m = 2$, $i_a = i_k = ½$ and selection for cooperation is as optimal as kin selection. However, evolution was trapped by PD for $m \geq 3$. By constructing the individual fitness of $i_k$ and $i_a$ viruses in pure and mixed groups of size $m \geq 3$, we found that the resulting fitness values conformed to a PD payoff matrix (Fig. 2d-f). Thus, our first model with linear tradeoffs was unable to evolve cooperation and remained trapped into the PD domain.

Our examination of a non-linear tradeoff was motivated by the molecular biology of VSV DI particles. Although a linear tradeoff was justified for replication and transcription (Fig. 1a), DI particles are more than just defectors with $i = 1$ and producing no public goods ($1 - i = 0$). Once a defector evolves to produce zero public goods, it can delete the coding sequences and replace its replication and transcription site with a replication-only site (Fig. 1b). These changes introduce a non-linear tradeoff because such an ultra-defector is able to make $i = 1 + e$ copies of its genome, where $e$ is the amount gained by having to replicate a smaller genome and not having to spend time on transcription (Fig. 1c). The value of $e$ is a constant representing a cap to the non-linear gain. Thus, $i$ is now able to evolve in the interval $i \in [0, 1 + e]$ through mutations. Because it is now also possible that $i > 1$, the new constraint $1 - i \geq 0$ was added to the model to prevent public goods from being produced at a negative rate.

The addition of a non-linear tradeoff and $i > 1$, altered qualitatively the evolutionary dynamics of our model (Fig. 3a). Letting $m = 8$ and $e = ½$, we started with a monomorphic population with $i = ½$ and allowed evolution to proceed with mutations. The population quickly evolved to a steady state of $i_a$ (Eq [2]) as we had reported for a linear model and PD (cf. Fig. 2b; $m = 8$). However, as mutations

accumulated, the population bifurcated into a lineage of ultra-defectors and one of ultra-cooperators. In the ultra-defectors, $i$ evolved upwards until it equaled the cap of $1 + e$, while in the ultra-cooperators it evolved downwards to the kin selected optimum of $i_k = ½$. Note that the evolution of ultra-cooperators occurs only after the ultra-defectors begin to increase in frequency. Thus, a mutant ultra-defector must have a minimum value of $i$ in order to invade the steady state $i_a$ population. By using equation [1] to estimate the fitness of the DI mutant in the $i_a$ population, and assuming that the mutant is at a low frequency, the minimum needed by the ultra-defector was found to be

$$i_d = 1 + \frac{1}{m\,(m-2)} \qquad [3]$$

(see Methods for the analytical derivation; equation [M6]). The bifurcation and the evolution of the ultra-defector also allow the population finally to escape PD and transition into SD. By constructing the individual fitness of $i_k$ and $i_d$ viruses in pure and mixed groups of size $m \geq 3$, the resulting fitness values conformed to a SD payoff matrix (Fig. 3b-c).

Equations [2] and [3] can be used to partition parameter space and constructing a landscape for the evolution of cooperation. As the model has only two parameters, let $1 + e$ and $m$ be the $y$ and $x$ axes, in which case equation [3] delineates the boundary between PD and SD (Fig. 4a). Thus, for all values of $m \geq 3$, PD evolves if $1 + e < i_d$, and SD evolves if $1 + e > i_d$. If $m$ =1 or 2, kin selection is sufficiently strong and the optimum $i_k = ½$ evolves. Note that when $e = 0$, the model reverts to the linear form and the outcome is PD as described by equation [2]. By plotting the amount of public goods produced as the response variable on the $z$ axis, a landscape for the evolved level of cooperation as a function of $1 + e$ and $m$ is generated (Fig. 4b). Public goods are produced maximally by kin selection, but nearly equivalent amounts are produced by SD. Moreover, as $1 + e$ and $m$ are increased in SD, ultra-cooperators are selected to make even more public goods to make up for consumption of the progressively stronger and more numerous ultra-defectors. Indeed, it can be shown mathematically that as $1 + e$ increases, $i_a$ tends to $i_k = ½$ (see Methods; analysis of equation [M7]). However, because the frequency of individuals producing public goods is not equal (Fig. 4c), we also examined the landscape for the mean production of public goods as a response variable (Fig. 4d). Because the frequency is low for high values of $1 + e$ and $m$, the highest mean production, outside of kin selection, is situated centrally, in the SD region, and just beyond the $i_d$ boundary.

The evolution of cooperation is a problem partly because it has been easier to identify the barriers to the process rather than solutions. PD presented an obstacle, but it was not even clear that escaping PD would promoted cooperation. The cooperator could evolve to resist better the defector, but that only

makes the goods less public, as did reciprocation and kin selection. SD was recognized as an advanced form of cooperation, but we knew little about its evolutionary maintenance, origin, and link to PD and kin selection. Our model resolves many of these issues by mapping the evolution of cooperation onto two parameters, group size and the magnitude of the non-linear gain to an ultra-defector. On this parametric space, increasing group size alone is sufficient for driving the evolution of cooperation from kin selection to PD and to SD. We show that the transition to SD results from the splitting of the population into lineages of ultra-defectors and ultra-cooperators. However, the split is triggered by the initial evolution of more defection, rather than more cooperation. If the tradeoff between defection and cooperation is linear, PD traps the population because the evolution of more defection, and the split, is prevented. With a non-linear tradeoff, more defection and the ultra-defector are able to evolve. Once the ultra-defector increases in frequency, the cooperator is selected to make even more public goods and to evolve into the ultra-cooperator of SD. The best ultra-cooperators make nearly as much public goods as kin selected individuals. Our work is theoretical, but it is well grounded into the biology of RNA viruses and their DIs. We hope that our work will stimulate additional work on RNA viruses or other organisms that produce public goods as model systems to explore social evolution.

**References**


1. Turner, P. E., Burch, C. L., Hanley, K. A. & Chao, L. Hybrid frequencies confirm limit to coinfection in the RNA bacteriophage φ6. *J. Virol.* **73**, 2420-2424 (1999).

2. Whitaker-Dowling, P. A., Youngner, J. S., Widnell, C. C. & Wilcox, D. K. Superinfection exclusion by vesicular stomatitis virus. *Virology* **131**, 137-143 (1983).

3. Bergua, M. *et al*. A viral protein mediates superinfection exclusion at the whole organism level but is not required for exclusion at the cellular level. *J. Virol*. **88**, 11327-11338 (2014).

4. Doebeli, M. & Hauert, C. Models of cooperation based on the Prisoner's Dilemma and the Snowdrift game. *Ecol. Lett*. **8**, 748-766 (2005).

5. Doebeli, M., Hauert, C. & Killingback, T. The evolutionary origin of cooperators and defectors. *Science* **306**, 859-62 (2004).

6. Kummerli, R. *et al*. Human cooperation in social dilemmas: comparing the Snowdrift game with the Prisoner's Dilemma. *Proc. R. Soc. B* **274**, 2965-2970 (2007).

7. Turner, P. E. & Chao, L. Prisoner's dilemma in an RNA virus. *Nature* **398**, 441-443 (1999).

8. Turner, P. E. & Chao, L. Escape from Prisoner's Dilemma in RNA phage φ6. *Am. Nat*. **161**, 497-505 (2003).

9. Holland, J. J. Generation and replication of defective viral genomes. In *Fundamental Virology*. (eds. Fields, B. N. & Knipe, D. M.) 6.77-6.99 (Raven Press, New York, 1986).

10. Dixit, N. M. & Perelson, A. S. Multiplicity of human immunodeficiency virus infections in lymphoid tissue. *J. Virol*. 78, 8942-8945 (2004).

11. Gutiérrez, S. *et al*. Dynamics of the multiplicity of cellular infection in a plant virus. *PLoS Pathog*. **6**, e1001113 (2010).

12. Giachetti, C. & Holland, J. J. Vesicular stomatitis virus and its defective interfering particles exhibit *in vitro* transcriptional and replicative competition for purified L-NS polymerase molecules. *Virology* **170**, 264-7 (1989).

13. Horodyski, F. M. & Holland, J. J. Reconstruction experiments demonstrating selective effects of defective interfering particles on mixed populations of vesicular stomatitis virus. *J. Gen. Virol*. **65**, 819-23 (1984).

14. Kolakofsky, D. Isolation and characterization of Sendai virus DI-RNAs. *Cell* **8**, 547-55 (1976).

15. Nayak, D. P., Sivasubramanian, N., Davis, A. R., Cortini, R. & Sung, J. Complete sequence analyses show that two defective interfering influenza viral RNAs contain a single internal deletion of a polymerase gene. *Proc. Natl. Acad. Sci. USA* **79**, 2216-20 (1982).

16. Nonoyama, M. & Graham, A. F. Appearance of defective virions in clones of reovirus. *J. Virol*. **6**, 693-4 (1970).

17. Stampfer, M., Baltimore, D. & Huang, A. S. Ribonucleic acid synthesis of vesicular stomatitis virus. I. Species of ribonucleic acid found in Chinese hamster ovary cells infected with plaque-forming and defective particles. *J. Virol*. **4**, 154-61 (1969).

18. Weiss, B., Goran, D., Cancedda, R. & Schlesinger, S. Defective interfering passages of Sindbis virus: nature of the intracellular defective viral RNA. *J. Virol*. **14**, 1189-98 (1974).

19. Cole, C. N. & Baltimore, D. Defective interfering particles of poliovirus. 3. Interference and enrichment. *J. Mol. Biol*. **76**, 345-61 (1973).

**Acknowledgements** We dedicate this paper to the memory of John J. Holland, who first brought the authors to UCSD and taught us so much about defective viral genomes and virus evolution. Work was supported by grants to L.C. from the National Science Foundation (DEB-1354253) and to S.F.E. from Spain's Ministries of Education, Culture and Sport (*Salvador de Madariaga* Program PRX15/00149) and Economy and Competitiveness (BFU2015-65037-P), Generalitat Valenciana (PROMETEOII/2014/021) and the European Commission 7th Framework Program EvoEvo Project (grant ICT-610427).

**Author Contributions** L.C. and S.F.E. conceived the study, designed and analyzed the model, collected the data, and wrote the manuscript.

**Author Information** The authors declare no competing financial interests. Correspondence and requests for materials should be addressed to LChao@ucsd.edu (L.C.). or sfelena@ibmcp.upv.es (S.F.E.)

## METHODS

**Monte Carlo model for simulating of evolution in viral populations.** A population of size *N* viruses was constructed by assigning a starting value of *i* to each virus. The assigned value could be random or deliberately chosen to explore different starting scenarios. The population was then divided into *N*/*m* groups of size *m* and the fitness of individual viruses was determined with equation [1]. To create the population for the next generation, the current population was sampled *N* times with replacement to ensure a constant population size. The sampling was biased by using the normalized fitness values of each virus as their probability of being chosen. This bias introduces natural selection and evolution could thus be modeled and followed over generations. Whenever desired, mutations were introduced by changing individual values of *i* with a probability of $0 < u < 1$. If mutations were not desired, a value of $u = 0$ was used instead. If a virus was to be mutated, its *i* value was changed by an amount randomly drawn from a Gaussian distribution with a mean zero and a specified standard deviation. All simulations were coded in R version 3.2.4 computer lenguage.

**Analytical solution of equation [2].** Let *j* be the investment of a mutant virus on reproduction and *i* the investment of the wild type virus and $j > i$. The fitness of a wild type virus in a population all formed by wild type viruses can be computed using equation [1]. In such case the burst size would be $b_{wt} = (1 - i)/m$ and the total reproductive effort $g_{wt} = i/m$ and thus

$$w_{wt} = \frac{1-i}{m}. \qquad \text{[M1]}$$

Now let imagine that a defector mutant that invests $j > i$ into reproduction appears in a population of $m - 1$ wild type viruses. The fitness of this mutant can be calculated using equation [1] but now considering that $b_{def} = [(m-1)(1-i) + 1 - j]/m$ and $g_{def} = [(m-1)i + j]/m$:

$$w_{def} = \frac{j[(m-1)(1-i)+1-j]}{m[(m-1)i+j]}. \qquad \text{[M2]}$$

Coexistence of both genotypes would occur if and only if $w_{wt} = w_{def}$. If $w_{wt} < w_{def}$, then the defector mutant will invade, whereas the opposite condition means that invasion is not possible. Combining equations [M1] and [M2] and after some algebra, we found that there are two different values of $j$ that satisfy the coexistence condition: $j = i$ and $j = (1 - i)(m - 1)$. These two lines correspond to pairs of values $(i, j)$ in which defector mutant and wild type have equal fitness. The intersection of this two fitness isoclines results in the equilibrium condition shown in equation [2]:

$$i_a \equiv \hat{\imath} = \hat{\jmath} = 1 - \frac{1}{m}.$$

The linear stability of this fixed point we evaluated by constructing the Jacobian matrix of the system formed by equations [M1] and [M2], which is given by

$$J(i,j) = \begin{pmatrix} \frac{\partial w_{wt}}{\partial i} & \frac{\partial w_{wt}}{\partial j} \\ \frac{\partial w_{def}}{\partial i} & \frac{\partial w_{def}}{\partial j} \end{pmatrix} = \begin{pmatrix} -\frac{1}{m} & \frac{j(1-m)}{[j+i(m-1)]^2} \\ 0 & \frac{i(m-1)}{[j+i(m-1)]^2} - \frac{1}{m} \end{pmatrix}.$$

The two eigenvalues for the fix point $(\hat{\imath}, \hat{\jmath})$ are $\lambda_1 = 1/m^3$ and $\lambda_2 = -1/m$. Since $\lambda_1 > 0$ and $\lambda_2 < 0$ $\forall$ $m > 0$, the fix point takes the form of a saddle and is thus instable.

**Analytical solution of equation [3].** The solution is obtained by exploring the conditions in which a DI mutant will invade a population at the equilibrium specified by equation [2]. Substituting $i$ by the equilibrium condition given by equation [2] into equations [M1] and [M2] and recalling that DIs do not contribute to the production of common goods and have an investment in reproductive effort $1 + e > i$, we obtain after some algebraic work the following fitness equations for wild type and DI, respectively:

$$w_{wt} = \frac{1}{m^2} \qquad \text{[M3]}$$

and

$$w_{DI} = \frac{(1+e)(m-1)}{m[(m-1)^2+m(1+e)]}. \qquad \text{[M4]}$$

Making $w_{wt} = w_{DI}$ and solving for $1 + e$, we found the $1 + e$ value at which wild type and DI viruses will coexist (equation [3]):

$$i_d \equiv 1 + e = 1 + \frac{1}{m(m-2)}.$$

**Constructing payoff matrixes for PD and SD.** Payoff values of $R$, $T$, $S$, and $P$ in a game theory matrix traditionally represent interactions between two individuals rather than between many in a large group.

Because our models consider groups of size $m$ that can be much larger than two, we adapted the payoff matrix to represent individual fitness values in populations with only cooperators, only defectors, one cooperator invading a large population of defectors, and one defector invading a large population of cooperators. The fitness of the invading cooperator, which equals the value the virus has when it is alone in a group with $m - 1$ defectors, represents $R$. The fitness of the invading defector represents $T$, or the value when it is alone in a group of $m - 1$ cooperators. The fitness of a cooperator in a population with only cooperators represents $R$, or the value when it is in a group with $m$ cooperators. The fitness of a defector in a population with only defectors represents $T$, or the value when it is in a group with $m$ defectors. A payoff matrix adapted to larger groups retains the predictive properties for an ESS analysis. If $T > R$, a defector is able to invade a population of cooperators. If $S > P$, a cooperator is able to invade a population of defectors, which is one of the requirements for SD. All fitness values were based on equation [1].

**Numerical solutions to obtaining the evolved values, means and frequency of *i*.** Solutions were derived for the parameter space represented in Figs. 4a-d. For a given pair of parameters $m$ and $1 + e$, the evolved $i$ was found by searching over the range of [0, 1] the value of $i$ that conferred a higher fitness than the neighboring values $i \pm \delta$. A value of $\delta = 0.001$ was used for all evaluations. The derived solutions are therefore the evolutionarily stable outcomes. For a comparison to determine the match between these numerical and the Monte Carlo results, see Extended Data. The search code was written in R version 3.2.4 computer language.

**Model generalization for any *m* group size and composition of virus and DIs.** Next, we will develop expressions to analyze the equilibrium conditions for the general case where group size, $m$, is randomly distributed and the metapopulation contains a frequency of $p$ virus and $1 - p$ DIs. Recalling that group size is Poisson distributed with an expected rate $\mu$ and that the probability that a group of size $m$ contains $x$ cooperators (and thus $m - x$ defectors) conforms to a Binomial probability distribution, then the fitness of the wild type and DI viruses in the population are given by the following expressions, respectively:

$$w_{wt} = \sum_{m=0}^{\infty} \frac{\mu^m}{m!} e^{-\mu} \frac{\sum_{x=0}^{m} P(x)b(x)g(x)}{\sum_{x=0}^{m} xP(x)} \qquad \text{[M5]}$$

$$w_{DI} = \sum_{m=0}^{\infty} \frac{\mu^m}{m!} e^{-\mu} \frac{\sum_{x=0}^{m} P(x)b(x)[1-g(x)]}{\sum_{x=0}^{m} (m-x)P(x)}, \qquad \text{[M6]}$$

where $P(x) = \binom{m}{x} p^x (1-p)^{m-x}$ is the probability of having $x$ wild type viruses in a group of size $m$, $b(x) = x(1-i)/m$ the per capita investment in the production of common goods in a coinfection group of size $m$ that contains $x$ wild types and $g(x) = xi/[xi + (m-x)(1+e)]$ the relative investment in

genome replication in the same group. Notice that the denominator in [M5] is the expected value of the Binomial distribution $mp$ and, likewise, the denominator in expression [M6] is $m(1 - p)$. In the equilibrium $w_{wt} = w_{DI}$, and we have

$$\frac{\sum_{x=0}^{m} P(x)b(x)g(x)}{\sum_{x=0}^{m} P(x)b(x)[1-g(x)]} = \frac{p}{1-p},$$

which, after replacing $P(x)$, $b(x)$ and $g(x)$ by their actual values, is equivalent to

$$\sum_{x=0}^{m} \frac{\binom{m}{x} p^x (1-p)^{m-x} x^2}{xi+(m-x)(1+e)} \Big/ \sum_{x=0}^{m} \frac{\binom{m}{x} p^x (1-p)^{m-x} (m-x)x}{xi+(m-x)(1+e)} = \frac{(1+e)p}{i(1-p)}. \qquad \text{[M7]}$$

Equation [M7] can be solved analytically for any value of $m \geq 2$ to obtain the equilibrium frequency of the cooperator virus as a function of $i$ and $e$, namely $\hat{p}(i, e|m)$. For instance, in the case $m = 3$, the equilibrium frequency for the cooperator virus is given by $\hat{p}(i, e|3) = i(1 + e + 2i)/[2(1 + e)(1 + e - i)]$, which takes positive values for any $i < 1 + e$ value. Linear stability analysis shows that the two eigenvalues of the Jacobian matrix $J(i, e) = \begin{pmatrix} \partial w_{wt}/\partial i & \partial w_{wt}/\partial e \\ \partial w_{DI}/\partial i & \partial w_{DI}/\partial e \end{pmatrix}$ evaluated at the fix point $\hat{p}(i, e|3)$ are $\lambda_1 < 0$ and $\lambda_2 > 0$, as corresponds to a unstable saddle fix point. For $m \geq 4$, $\hat{p}(i, e|m)$ is a complex polynomic function of $i$ and $e$, with at least one root in the interval [0, 1] that in every case corresponds to an unstable saddle point. Equation [M7] can also be solved numerically for every value of $m$ to find the frequency $p$ of cooperators in the population as a function of values of $i$ and $e$. The numerical analysis of equation [M7] generates a very interesting insight: for any given value of $m$ one can explore which values should take $i$ to hold the expected frequency of cooperators $\hat{p}(i, e|m)$ constant if the DIs take increasingly large values of $e$. It turns out that at the limit when $e \to \infty$, then $i \to ½$. This means that the optimal solution for a wild type virus in presence of an ultra-defector DIs would be to become itself and ultra-cooperator and invest 50% of its resources in the production of common goods.

**Figure 1 | Tradeoff between replication and transcription in VSV viruses and DIs.** **a**, Complete single stranded RNA genome of VSV with all required genes. After the (–) strand enters a host cell, the segment *z* serves as the initiation site for the synthesis of the (+) strand, which acts as both the messenger RNA and the replication template for the (–) strand. The segment *a'* acts as the initiation site for both transcription and replication and the (+) strand is therefore constrained to tradeoff between providing public goods and reproduction. **b**, Single stranded genomes of DI particles. This shortened DI genome is the most abundant type and it lacks the coding regions for genes needed for replication and infection. Additionally, the (+) and (–) strands become functionally equivalent and only capable of replication because their *a'* and *a* segments are replaced with *z* and *z'* segments, respectively. **c**, Linear and non-linear tradeoffs between replication and transcription in VSV. Following the model, a virus can allocate an amount of available resources $i$ to replication and $1 - i$ to transcription. In the absence of DIs, a linear tradeoff (----) is assumed between $i$ and $1 - i$ because a virus can only tradeoff by modulating the initiation site *a'* to favor either replication or transcription, $0 \leq i \leq 1$ and $0 \leq 1 - i \leq 1$. If $i = 1$ and $1 - i = 0$, *a'* has been modulated to promote only replication. With the evolution of DIs the tradeoff becomes nonlinear because DIs acquire an even higher replication by both foregoing transcription and being smaller and replication rate $i > 1$. To prevent $i$ from becoming infinity large, a replication cap of $1 + e$ was set (■), where $e \geq 0$ and $e = 0$ reverts to a linear tradeoff. Because $i > 1$ makes the transcription rate $1 - i$ negative, the tradeoff was bounded $1 - i \geq 0$. DIs with $i = 1 + e > 1$ were termed ultra-defectors.

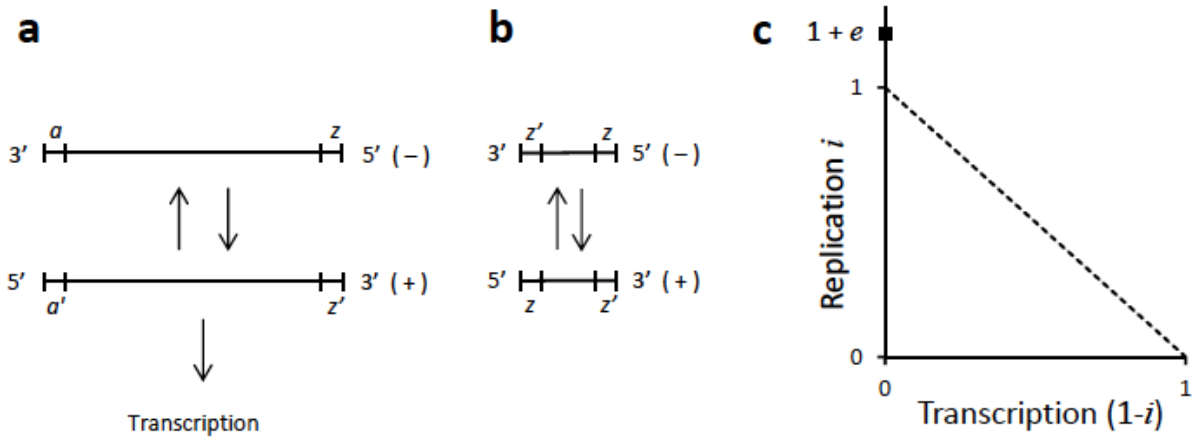

**Figure 2 | Linear tradeoff and the evolution of PD.** All populations evolved with a linear tradeoff and a Monte Carlo simulation with population size of $N$ = 1000, genomic mutation rate of $u$ = 0.2 and a Gaussian distribution of mutational effects with mean zero and standard deviation 0.005 (see Methods for additional details). **a**, Evolutionary changes with $m$ = 1. Grey areas represent all individual $i$ values over time in three independent populations started with $i$ = 0.8, 0.5 and 0.2. Black trace (——) represents mean $i$ values for population started with $i$ = ½. A value of $m$ = 1 serves as a control for the consequences of kin selection because all individuals in a group descend from one individual. The consequence of kin selection is that replication and the production of public goods evolves to the optimum of equaling each other, or $i_k = 1 - i_k = ½$. **b**, Traces of mean $i$ values for independent populations evolved with increasing values of $m$. **c**, Match of $i$ values predicted by analytical solution $i_a = 1 - 1/m$ and mean values evolved by Monte Carlo simulations. **d**, General payoff matrix representing PD. The payoffs are the fitness values reward $R$ when both players cooperate, temptation $T$ for one player to defect, sucker's payoff $S$ for the cooperator facing defection, and penalty $P$ for both players defecting. PD requires the rank order $T > R > P > S$. **e**, Fitness payoff matrix for $m$ = 2 (see Methods for matrix estimation). The population avoids PD because $R$ is the highest value. Cooperation is favored because group size is sufficiently small to allow kin selection. **f**, Fitness payoff matrix with $m$ = 3. The required PD rank order is satisfied. Optimal cooperation of $i$ = ½ is not possible with PD, and defection leads to the evolution of PD and the evolved value of $i_a = 1 - 1/m$ (equation [2]). **g**, Relationship between payoffs $T$, $R$, $P$, and $S$ with increasing $m$. Required rank order for PD is satisfied for all $m > 2$.

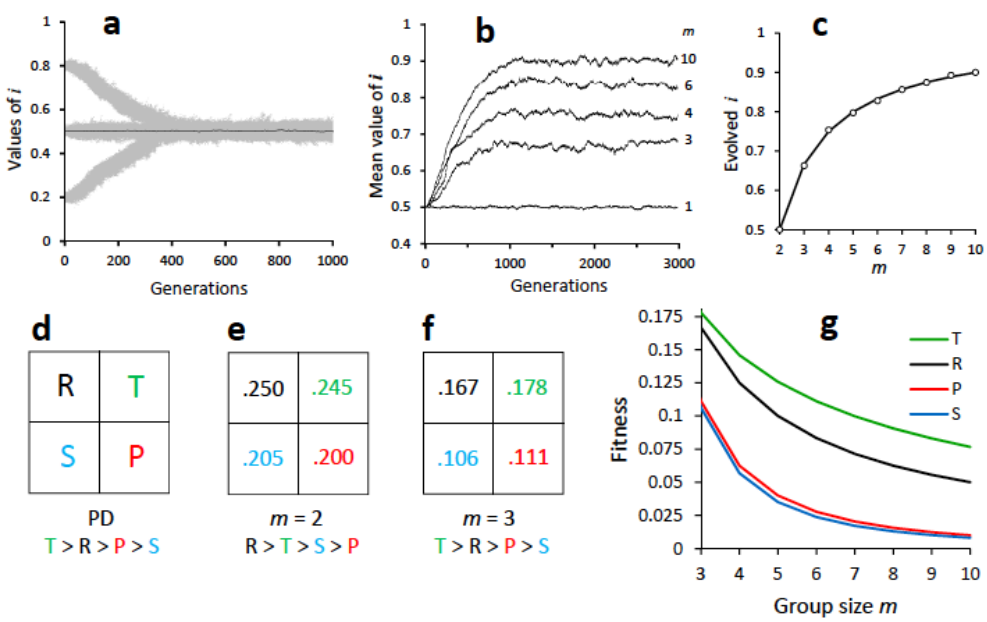

**Figure 3 | Nonlinear tradeoff and the evolution of SD.** All populations evolved with a nonlinear tradeoff ($e > 0$) via a Monte Carlo simulation using the same parameters as in Fig. 2, unless otherwise specified. **a**, Evolutionary changes with $m = 8$ and a replication cap of $1 + e = 1.5$. Grey areas represent all individual $i$ values over time in a population started with $i = 0.5$. Population evolves steadily higher $i$ values to $1 - 1/m = 7/8$ (equation [2]) and mutations increasing $i > 1$ surface at 1200 generations. At 1800 generations a mutant evolves into an ultra-defector with $i = 1.5$. In response to the evolution of the ultra-defector, the population splits into a second lineage of ultra-cooperators that evolves a lower replication rate $i$, or a higher rate of public good production of $1 - i$. **b**, General fitness payoff matrix representing SD with rank $T > R > S > P$ (see Fig. 2 for additional details). **c**, Payoff matrix for population and conditions in Fig. 2a (see Methods for matrix estimation). Rank matches requirement for SD. The population is polymorphic and ultra-cooperators and ultra-defectors coexist because ultra-defectors can invade a population of ultra-cooperators ($T > R$) and *vice versa* ($S > P$). **d**, Relationship between fitness payoffs $T$, $R$, $S$, and $P$ with non-linear tradeoffs $1 + e = 1.15$ and increasing $m$. The threshold for evolving SD is given by equation [3] or $1 + e > 1 + 1/[m(m - 2)]$, which is satisfied for $m \geq 4$. For $m = 3$, the threshold is not satisfied and the rank is PD because $1.15 < 1.33$. **e**, Relationship between fitness payoffs $T$, $R$, $S$, and $P$ with $m = 3$ and increasing replication cap $1 + e$. With $m = 3$, the threshold for evolving SD is 1.33 (▲) as in Fig. 2d. The rank is PD for $1 + e < 1.33$ and SD for $1 + e > 1.33$.

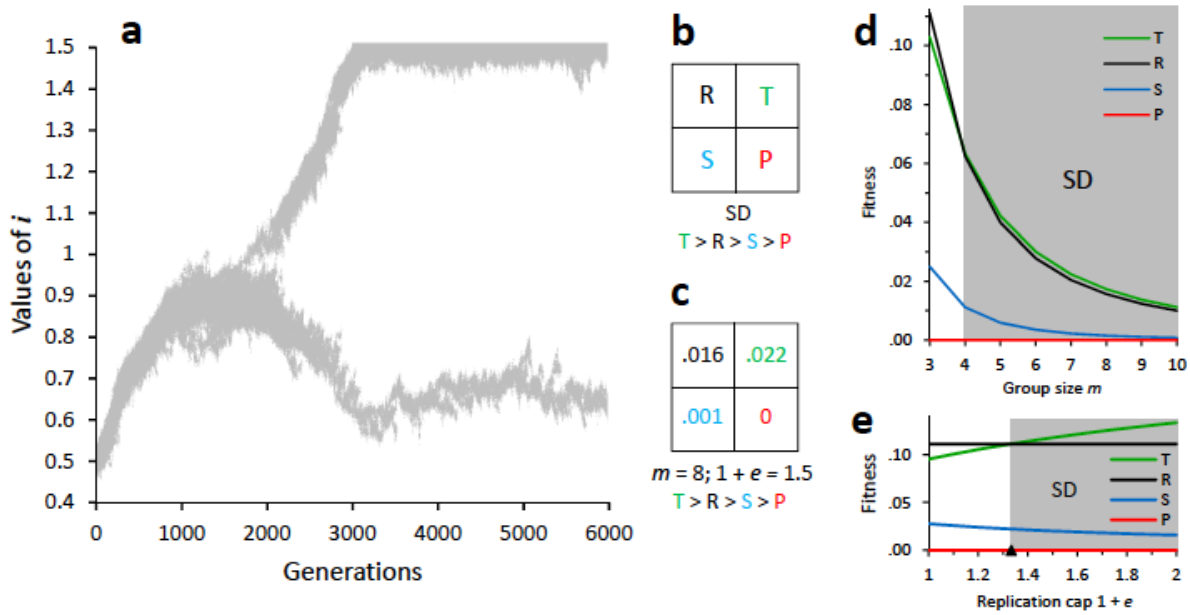

**Figure 4 | Parameter landscapes for the evolution of cooperation**. Plots are topographic representations of evolutionary outcomes projected onto the parameter space of group size $m$ and replication cap $1 + e$. All graphed outcomes were obtained as either analytical or numeric solutions and were also verified through comparisons to Monte Carlo simulations (see Methods). **a**, Parameter space leading to the evolution of kin selection, PD, and SD. Boundary for kin selection and PD is given by equation [2] and for PD and SD by equation [3]. **b**, Evolved maximal level of individual cooperation represented as the production of public goods $1 - i$. Values in the PD region are from equation [2]. Values in SD region are numerical solutions (see Methods) representing the production by ultra-cooperators. **c**, Frequency of individuals producing the maximal individual values in Fig. 2**b**. Kin selected and PD populations are monomorphic and all individuals produce maximally. SD populations are polymorphic and frequencies represent ultra-cooperators. **d**, Evolved mean level of individual cooperation $1 - i$ in populations. Because PD populations are monomorphic and ultra-defectors in SD populations do not produce public goods, the mean is the product of individual values and frequencies from Figs. 2b and 2c. A maximum value of 0.33 (+) was observed at $m = 3$ and $1 + e = 1.34$.

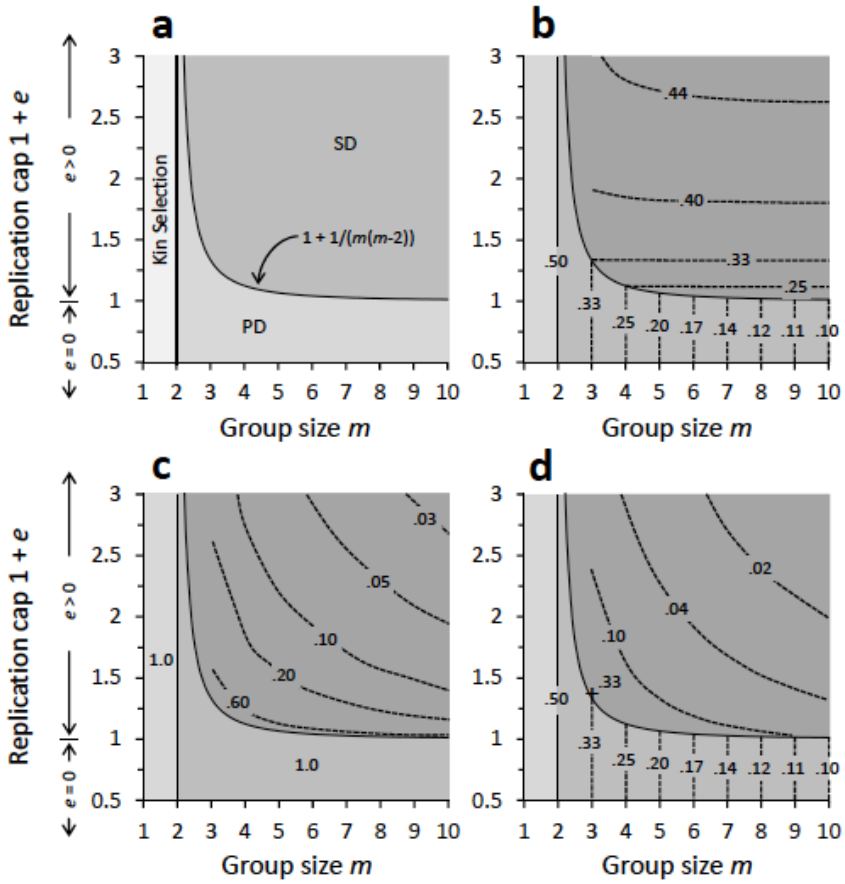

**Extended Data**
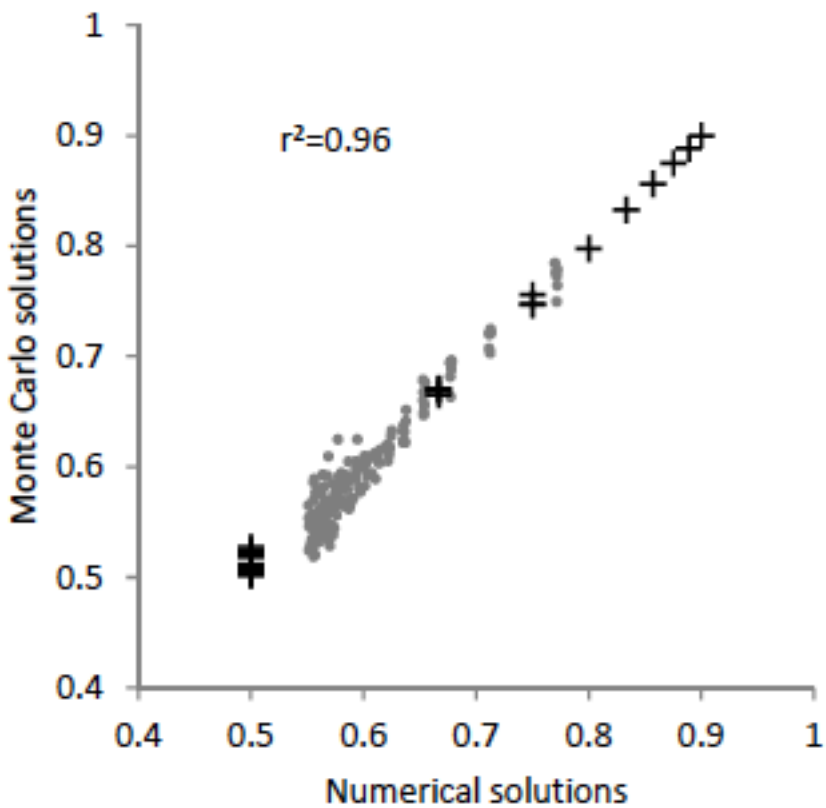
**Figure E1 | Comparing Monte Carlo and numerical solutions for evolved values of *i*.** Solutions obtained as described in Methods. Individual points represent *i* values obtained by the Monte Carlo (MC) and numerical solutions. MC simulations were run for 10,000 generations with population size of $N = 500 \cdot m$, where $m$ is group size, and a mutation rate of $u = 0.2$ and a Gaussian distribution of mutational effects with mean zero and standard deviation 0.005. Populations generally reach equilibrium values after 1000 generations (Fig. 2a). Reported values of *i* are the mean value at the last generation. The parameter space represented in Figs. 4a-d was explored by letting $m$ range from 2, 3, 4, …, 10 and $1 + e$ from 1, 1.1, 1.2, …, 3.0. Values of *i* corresponding to PD (+) and SD (●). The match between MC and numerical solutions yielded a value of $r^2 = 0.96$.